Discovery of Potent Antagonists of the Interaction between Human Double Minute 2 and Tumor Suppressor p53

Carlos García-Echeverría,*,† Patrick Chène,† Marcel J. J. Blommers,‡ and Pascal Furet*,†

Oncology Research and Core Technologies, Novartis Pharma Inc., CH-4002 Basel, Switzerland

Received December 8, 1999

Introduction. The p53 tumor suppressor gene is a multifunctional protein that regulates cell proliferation by induction of growth arrest or apoptosis in response to DNA damage and/or stress stimuli.[1] Despite the high frequency and susceptibility with which this protein is mutated during neoplastic transformation, a substantial proportion of cancer cells express wild-type p53, but it seems likely that in these cells p53 is inactivated. Among the known mechanisms by which the tumor suppressor functions of p53 can be abrogated,[2] we are interested in the regulation of p53 by the human double minute 2 (hdm2) oncoprotein.[3] The hdm2 protein binds to the transactivation domain of p53[4] and downregulates its ability to activate transcription; in turn, p53 activates the expression of the hdm2 gene in an autoregulatory negative feedback loop.[2−4] Inhibition of p53 by hdm2 has been observed in tumors where gene amplification and other alterations can result in elevated hdm2 (e.g., one-third of soft tissue sarcomas).[3c,5] Recently, an additional mechanism by which hdm2 can regulate p53 response has been reported. hdm2 targets p53 for degradation by the ubiquitin pathway.[6] If this pathway operates in tumor cells containing low levels of p53, then disruption of the p53/hdm2 protein−protein interaction should lead to accumulation of p53 and activation of p53 responsive reported genes. The disruption of the p53/hdm2 protein−protein interaction is therefore an attractive approach for cancer therapy because it provides the possibility to regulate the threshold of the p53 response with therapeutic agents.

As part of our drug discovery program to identify antagonists of the p53/hdm2 protein−protein interaction, we have attempted to determine the amino acid specificities of hdm2's binding pockets in order to establish a pharmacophore model for this protein−protein interaction. This work has resulted in the identification of highly potent peptide antagonists.

Results and Discussion. The p53/hdm2 complex was initially studied with a series of monoclonal antibodies to identify the region of p53 that interacts with hdm2 and vice versa. Mapping of the hdm2-binding site on p53 was carried out using synthetic peptide libraries derived from the N-terminal part of p53.[7a] The active peptides defined the consensus hdm2-binding site on p53 to be Thr[18]-Phe-Ser-Asp-Leu-Trp[23], but this hexapeptide had a low binding affinity for hdm2 (IC_{50} = 700 μM).[8] To find novel high-affinity ligands for hdm2 that are able to block the interaction of hdm2 with p53, we screened phage display peptide libraries.[9] The most active peptide obtained (peptide **2**; Table 1) showed a 28-fold greater inhibition of the p53/hdm2 interaction than the wild-type p53-derived peptide (peptide **1**; Table 1). More detailed information on the amino acid requirements for a potent peptide inhibitor was obtained by synthesizing truncated versions of peptide **2** and testing these peptides in our in vitro assay.[8] In this competition assay, the ELISA plates were coated with GST-hdm2. After preincubation with different amounts of peptide, full-length p53 was added and the fraction of p53 bound to hdm2 was detected with a series of antibodies (Figure 1; see Supporting Information for additional experimental details). The truncation series included sequences from 6- to 11-mers. While all 6- and 7-mer peptides were poor inhibitors of the p53/hdm2 interaction, an 8-mer peptide (peptide **3**; Table 1) was identified as the minimal sequence retaining micromolar affinity for hdm2. This peptide was our starting point in the optimization process.

The X-ray structure of the N-terminal domain of hdm2 bound to a 15-mer wild-type p53-derived peptide[10a] revealed a deep hydrophobic cleft to which the peptide binds as an amphipathic α-helix. In addition to this structural motif, a type I β-turn conformation involving Trp[23], Glu[24], Gly[25], and Leu[26] was identified. Before introducing any modifications into the sequence of peptide **3**, we studied the conformation of peptide **2** in solution to determine if this peptide has a preorganized conformation in its unligated form. The circular dichroism (CD) and nuclear magnetic resonance (NMR) studies (data not shown) revealed that peptide **2** has an extended or random coil conformation under physiological conditions. With this information in hand, we decided to modify peptide **3** by replacing the residues that, according to the X-ray structure of the ligand-bound hdm2 protein, do not interact or seem to have a weak interaction with the protein (e.g., residues 20, 21, 24, and 25) with α,α-disubstituted amino acids. These amino acids are known to stabilize α- and 3_{10}-helices in short peptide motifs,[11] and we posited that the incorporation of such building blocks into peptide **3** should favor the formation of a conformation close to the one observed for the ligand-bound wild-type p53-derived peptide.[10a] Conformationally restricted peptides that adopt ligand-binding conformations are supposed to be entropically advantaged for binding to their target. The best result was obtained when Asp[21] and Gly[25] were replaced with α-aminoisobutyric acid (Aib) and 1-aminocyclopropanecarboxylic acid (Ac_3c), respectively (peptide **4**; Table 1).[12] These substitutions only result in a 4-fold increase in the hdm2-binding affinity of the peptide, but NMR experiments in aqueous media confirmed that the conformational restrictions imposed by the presence of α,α-disubstituted amino acids in the peptide sequence induce p53-binding conformations. On the basis of the NOE signals obtained (Table 2), a model of the conformation of peptide **4** in solution was constructed using

* To whom correspondence should be addressed. Phone: 41 61 696 10 94 (C.G.-E.) and 41 61 696 79 90 (P.F.). Fax: 41 61 696 62 46. E-mail: carlos.garcia-echeverria@pharma.novartis.com and pascal.furet@pharma.novartis.com.

† Oncology Research.

‡ Core Technologies.

10.1021/jm990966p CCC: $19.00
Published on Web 08/05/2000

Table 1. Inhibitory Potential of hdm2-Binding Peptides in a p53/hdm2 (GST-hdm2$^{1-188}$) Competition Assay[a]

entry	sequence	IC_{50} (nM)[b]
1	Ac-Gln^{16}-Glu-Thr-Phe-Ser-Asp^{21}-Leu-Trp-Lys-Leu-Leu-Pro^{27}-NH_2	8673 ± 164
2	Ac-Met-Pro-Arg-Phe^{19}-Met-Asp-Tyr-Trp-Glu-Gly-Leu^{26}-Asn-NH_2	313 ± 10
3	Ac-Phe^{19}-Met-Asp-Tyr-Trp-Glu-Gly-Leu^{26}-NH_2	8949 ± 588
4	Ac-Phe^{19}-Met-Aib-Tyr-Trp-Glu-Ac$_3$c-Leu^{26}-NH_2	2210 ± 346
5	Ac-Phe^{19}-Met-Aib-Pmp-Trp-Glu-Ac$_3$c-Leu^{26}-NH_2	314 ± 88
6	Ac-Phe^{19}-Met-Aib-Pmp-6-F-Trp-Glu-Ac$_3$c-Leu^{26}-NH_2	14 ± 1
7	Ac-Phe^{19}-Met-Aib-Pmp-6-Me-Trp-Glu-Ac$_3$c-Leu^{26}-NH_2	10 ± 1
8	Ac-Phe^{19}-Met-Aib-Pmp-6-Cl-Trp-Glu-Ac$_3$c-Leu^{26}-NH_2	5 ± 1

[a] IC_{50} concentration to inhibit the binding of human wild-type p53 to GST-hdm2$^{1-188}$ (see Figure 1 and Supporting Information for a description of this assay). The errors quoted correspond to the standard error in the fits of the data. [b] The activities reported for these peptides correspond to the ones observed for the most active epimer (racemic 6-substituted tryptophan derivatives were used in the synthesis and the two epimers were separated to homogenity by preparative reversed-phase MPLC, see Supporting Information). On the basis of the activity observed for Ac-Phe-Met-Aib-Pmp-D-Trp-Glu-Ac$_3$c-Leu-NH_2 (IC_{50} = 138 ± 27 μM; 439 times less active than peptide **5**) and our computational studies, we can assume that the configuration of the 6-substituted tryptophans in the active epimers is L.

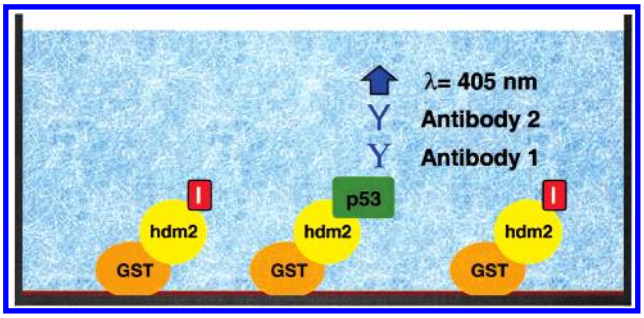

Figure 1. In vitro assay to determine the inhibiton of the p53/hdm2 (GST-hdm2$^{1-188}$) protein−protein interaction by synthetic peptides.

Table 2. List of NOEs Collected by ROESY and Used as Input in the Distance-Geometry Calculations (peptide **4**)

hydrogens		NOE signal[a]	hydrogens		NOE signal[a]
Phe H$^{\alpha}$	Phe H$^{\delta}$	s	Trp NH	Trp H2	w
Phe H$^{\alpha}$	Tyr H$^{\delta}$	w	Trp H$^{\alpha}$	Trp H4	s
Met H$^{\alpha}$	Trp NH	w	Trp H$^{\alpha}$	Trp H2	s
Met H$^{\alpha}$	Trp H2	m	Trp H$^{\alpha}$	Leu H$^{\beta}$	w
Tyr NH	Tyr H$^{\delta}$	w	Trp H$^{\alpha}$	Leu H$^{\gamma}$	w
Tyr H$^{\alpha}$	Ac$_3$c NH	w	Trp H$^{\alpha}$	Leu H$^{\delta}_2$	w
Tyr H$^{\delta}$	Trp H2	w	Trp H2	Leu H$^{\delta}_2$	w
Tyr H$^{\epsilon}$	Leu H$^{\delta}$	w	Leu H$^{\alpha}$	Leu H$^{\delta}_2$	m

[a] Upper bounds of 2.7, 3.3, and 5.0 Å were set for strong (s), medium (m), and weak (w) NOEs, respectively. The ROESY experiments with peptide **4** (c = 3.2 mM) were performed in aqueous solution (95% H_2O, 5% D_2O), 10 mM sodium phosphate, 100 mM NaCl, pH 6.0 (T = 0 and 20 °C). See Supporting Information for additional experimental details.

distance-geometry and restrained molecular dynamics (Figure 2). In most of the 100 structures generated, the hydrophobic amino acids Phe^{19}, Tyr^{22}, Trp^{23}, and Leu^{26} form a continuous hydrophobic patch that resembles the bound conformation of the wild-type p53-derived peptide. The side chain of tryptophan stacks face-to-face with the side chain of phenylalanine, and the peptide backbone between these two residues adopts a helical conformation. This structural motif is followed at the C-terminus by a β-turn, which enables the side chain of leucine to establish hydrophobic contacts with the side chains of tryptophan and tyrosine. To evaluate the relevance of the generated structures, the temperature coefficients of the amide resonances ($\Delta\delta/\Delta T$), the difference of chemical shifts of Hα resonances with random coil values[13] or chemical shift index (CSI), and the coupling constants ($J_{H\alpha-HN}$) were measured for peptides **3** and **4** (Table 3). Apart from the small coupling constant $J_{H\alpha-HN}$ observed for Glu^{24} in peptide **4**, the NMR data are very similar. However, considering that a CSI < −0.1 ppm for three subsequent residues is an indication for helix propensity,[14] peptide **4** seems to have a higher helix propensity than peptide **3**. The strongest evidence for this propensity comes from the NOE data. Qualitative information about the populations of helical and extended conformations can be derived from Hα−HN NOE intensities. The sequential Hα−HN distance is about 3.5 Å in an α-helix and close to 2.2 Å in an extended chain. The intraresidual Hα−HN distance is 3.5 Å for both conformations. These Hα−HN NOEs are expected to be almost equally strong for a helical conformation because a small population of extended conformation would result in an increase of the sequential NOE intensity. Such increase in the sequencial NOE intensity is observed for peptide **3**, but not for peptide **4** (Table 3).

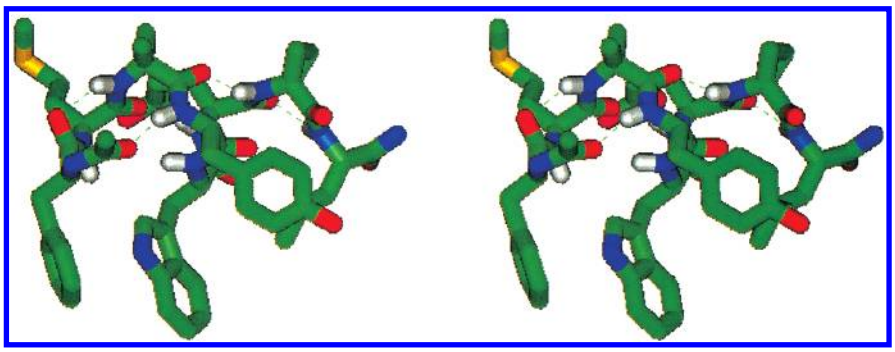

Figure 2. Stereoview of the solution structure of peptide **4** in aqueous media. The structure is a representative member (low energy) of a family of structures that was obtained by means of the distance restraints listed in Table 2; 100 structures were generated using the distance-geometry program DGII and were energy-minimized using Discover (see Supporting Information for experimental details).

Table 3. Temperature Coefficients of the Amide Resonances, Chemical Shift Index, Coupling Constants, and NOE Intensities Measured for Peptides **3** and **4**[a]

	peptide **3**					peptide **4**				
amino acid	$\Delta\delta/\Delta T \times 10^{-3}$ (ppm/K)	CSI (ppm)	$J_{H\alpha-HN}$ (Hz)	NOE Hα−HN(*i*,*i*)	NOE Hα−HN(*i*,*i*+1)	$\Delta\delta/\Delta T \times 10^{-3}$ (ppm/K)	CSI (ppm)	$J_{H\alpha-HN}$ (Hz)	NOE Hα−HN(*i*,*i*)	NOE Hα−HN(*i*,*i*+1)
Phe[19]	−8	−0.07	6.6	0.48	1.83	−8	−0.22	6.1	0.41	0.67
Met[20]	−7	−0.15	7.2	0.80	3.23	−6	−0.33	6.6	0.94	2.50
Asp[21]/Aib[21]	−6	−0.29	7.2	0.98	2.23	−6				
Tyr[22]	−7	−0.21	5.8	0.71	1.94	−6	−0.24	5.8	0.88	0.61
Trp[23]	−4	−0.20	6.4	0.58	2.16	−5	−0.21	6.2	0.29	0.24
Glu[24]	−4	−0.21	7.2	0.88	1.54	−4	−0.32	3.4	1.20	0.20
Gly[25]/Ac_3c[25]	−2	−0.25	5.1	2.33	1.22	−6				
Leu[26]	−6	−0.16	5.8	0.62	1.53	−3	−0.16	7.4	0.80	

[a] The NMR measurements were done in 10 mM phosphate buffer, pH 6.0, 100 mM NaCl, and 10 μM DSS (2,2-dimethyl-2-silapentane-5-sulfonate; internal reference) at 25 °C. NOE intensities were obtained using ROESY with mixing times of 100 ms. Temperature coefficients were obtained from NMR spectra recorded between 5 and 45 °C.

In the next round of optimization, we focused our attention on the interactions made by the side chains of tyrosine and tryptophan. A comprehensive replacement analysis of peptide **2** revealed that Phe[19], Tyr[22], Trp[23], and Leu[26] cannot be replaced by any of the other natural amino acids without a substantial loss of inhibitory capacity.[8] Using the X-ray crystal structure of the ligand-bound hdm2, a model of the complex of peptide **2** with hdm2 was constructed. Analysis of the contacts of peptide **2** with hdm2 identified the side chains of tyrosine and tryptophan as targets for chemical modification in order to improve the hdm2-binding affinity of the peptide. In particular, the proximity of the hydroxy group of the side chain of tyrosine to the amino group of the side chain of Lys[94] was noticed. This led to the idea of replacing tyrosine in peptide **4** by phosphonomethylphenylalanine in order to form a stabilizing salt bridge with the ϵ-amino group of Lys[94] (see Figure 3A). The 7-fold increase in binding affinity that resulted from this modification (peptide **5** compared to peptide **4**; Table 1) confirmed the validity of the design.[15] In addition, the phosphonate group increases the water solubility of an otherwise highly hydrophobic sequence.

A major increase in the binding affinity was obtained when chemical groups determined by molecular modeling were incorporated at the 6 position of the indole moiety of tryptophan. In the X-ray structure of the ligand-bound hdm2, the side chain of tryptophan is embedded in a deep hydrophobic pocket in which the bottom is formed by the side chains of Leu[57], Phe[86], Ile[99], and Ile[103]. Although the aromatic side chain of tryptophan fits tightly into the hydrophobic pocket, a careful analysis of the X-ray structure revealed that the indole group does not fill it completely. An empty space in the direction of the 6 position of the indole ring remains at the bottom of the pocket (Figure 3B). This space corresponds approximately to the volume of a methyl group or a chlorine atom, and the possibility to increase the binding affinity by establishing additional van der Waals interactions with the protein motivated the synthesis of peptides **6**−**8**. In accordance with our predictions, replacement of tryptophan by 6-substituted tryptophans resulted in a substantial increased in binding affinity, which nicely correlates with the size of the substituent and therefore with the occupancy of the hydrophobic pocket.[16]

In summary, structural information has been exploited to increase the hdm2-binding affinity of short peptide motifs derived from the N-terminal domain of the human wild-type p53 protein. Combining conformational constraints as selected by molecular modeling with functional groups that are able to establish additional electrostatic and van der Waals interactions with the hdm2 protein, we have been able to increase the hdm2-binding affinity of our initial peptide 1700-fold. Particularly interesting is the increase in binding affinity obtained by replacing tryptophan with 6-chlorotryptophan (IC_{50} = 314 nM versus IC_{50} = 5 nM, 63-fold). The new interactions identified and experimen-

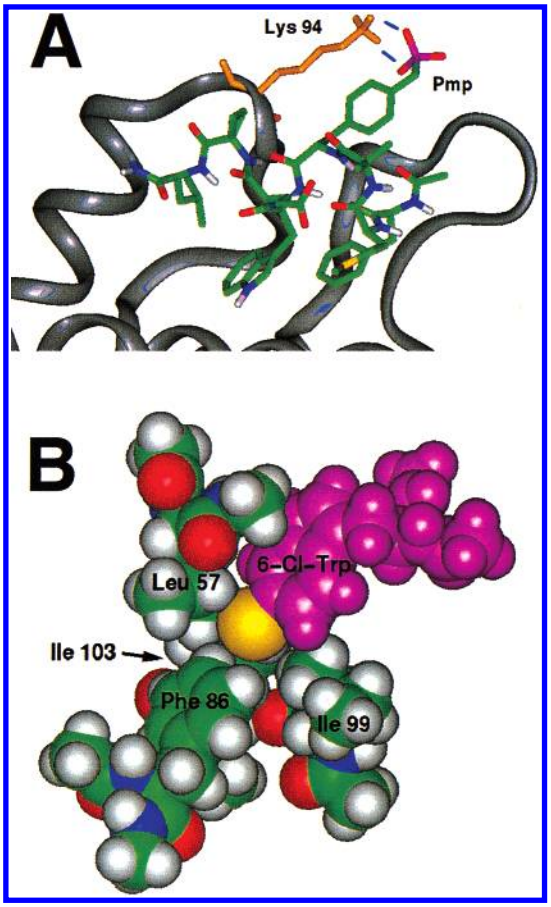

Figure 3. (A) Model of peptide **5** bound to hdm2. The designed salt bridge interaction between the phosphonate moiety of the phosphonomethylphenylalanine residue and the ϵ-amino group of Lys[94] is represented by two blue lines. (B) Partial representation of the hdm2 hydrophobic pocket occupied by tryptophan (CPK representation). The yellow sphere corresponds to the 6-chloro substituent of peptide **8** occupying the empty space at the bottom of the hydrophobic pocket.

tally confirmed in this work could be directly applied to the optimization of nonpeptidic leads or incorporated into the "de novo" design of antagonists of the p53/hdm2 protein−protein interaction. Furthermore, the work described above illustrates how the integration of multiple techniques in drug discovery can help in the formidable task to identify compounds capable of inhibiting therapeutically relevant protein−protein interactions.[17]

Acknowledgment. We thank D. Arz, R. Wille, and V. von Arx for technical assistance, J. Liebetanz for reading and correcting the manuscript, and Biosynth (Staad, Switzerland) for providing us with a free sample of 6-chloro-L,D-tryptophan.

Supporting Information Available: Synthesis and analytical data for compounds and a description of modeling work, NMR experiments, and biological assay. This material is available free of charge via the Internet at http://pubs.acs.org.

References

(1) For recent reviews on p53, see: (a) Kubbutat, M. H. G.; Vousden, K. H. Keeping on Old Friend under Control: Regulation of p53 stability. *Mol. Med. Today* **1998**, *4*, 250−256. (b) Harris, C. C. Structure and Function of the p53 Tumor Suppressor Gene: Clues for Rational Cancer Therapeutic Strategies. *J. Natl. Cancer Int.* **1996**, *88*, 1442−1455. (c) Arrowsmith, C. H.; Morin, P. New Insights into p53 Function from Structural Studies. *Oncogene* **1996**, *12*, 1379−1385. (d) Milner, J. The p53 tumour suppressor. In *Signal Transduction*; Heldin, C.-H., Purton, M., Eds.; Chapman & Hall: London, 1996. (e) Oliner, J. D. Discerning the Function of p53 by Examining its Molecular Interactions. *BioEssays* **1993**, *15*, 703−707. (f) Vogelstein, B.; Kinzler, K. W. p53 Function and Dysfunction. *Cell* **1992**, *70*, 523−526.

(2) Loss of p53 function through mutation in the p53 gene or other genomic alterations occurs in about half of all cancer cases: Greenblatt, M. S.; Bennett, W. P.; Hollstein, M.; Harris, C. C. Mutations in the p53 Tumor Suppresor Gene: Clues to Cancer Etiology and Molecular Pathogenesis. *Cancer Res.* **1994**, *54*, 4855−4878.

(3) hdm2 is the human counterpart of the mouse double minute 2 (mdm2) oncogene, which was originally identified as an amplified gene in a transformed mouse cell line: (a) Cahilly-Snyder, L.; Yang-Feng, T.; Francke, U.; George, D. L. Molecular Analysis and Chromosamal Mapping of Amplified Genes Isolated from a Transformed Mouse 3T3 Cell Line. *Somat. Cell. Mol. Genet.* **1987**, *13*, 235−244. (b) Momand, J.; Zambetti, G. P.; Olson, D. C.; George, D.; Levine, A. J. The mdm2 Oncogene Product Forms a Complex with the p53 Protein and Inhibits p53-Mediated Transactivation. *Cell* **1992**, *69*, 1237−1245. (c) Oliner, J. D.; Kinzler, K. W.; Meltzer, P. S.; George, D. L.; Vogelstein, B. Amplification of a Gene Encoding a p53-Associated Protein in Human Sarcomas. *Nature* **1992**, *358*, 80−83.

(4) Finlay, C. A. The mdm2 Oncogene can Overcome Wild-Type p53 Suppresion of Transformed Cell Growth. *Mol. Cell. Biol.* **1993**, *13*, 301−306.

(5) (a) Cordon, C. C.; Latres, E.; Drobnjak, M.; et al. Molecular Abnormalities of mdm2 and p53 Genes in Adult Soft Tissue Sarcomas. *Cancer Res.* **1994**, *54*, 794−799. (b) Ladanyi, M.; Cha, C.; Lewis, R.; Jhanwar, S. C.; Huvos, A. G.; Healey, J. H. Mdm2 Gene Amplification in Metastatic Osteosarcoma. *Cancer Res.* **1993**, *53*, 16−18. (c) Leach, F. S.; Tokino, T.; Meltzer, P.; et al. Mutation and mdm2 Amplification in Human Soft Tissue Sarcomas. *Cancer Res.* **1993**, *53*, 2231−2234. (d) Oliner, J. D.; Kinzler, K. W.; Meltzer, P. S.; Geroge, D. L.; Vogelstein, B. Amplification of a Gene Encoding a p53-Associated Portein in Human Sarcomas. *Nature* **1992**, *358*, 80−83. Amplification of hdm2 has been observed less often in other cancers, including gliobastomas, leukemias, esophageal carcinomas, and breast carcinomas.

(6) (a) Haupt, Y.; Maya, R.; Kazaz, A.; Moshe, O. Mdm2 Promotes the Rapid Degradation of p53. *Nature* **1997**, *387*, 296−299. (b) Kubbutat, M. H. G.; Jones, S. N.; Vousden, K. H. Regulation of p53 Stability by mdm2. *Nature* **1997**, *387*, 299−303.

(7) (a) Picksley, S. M.; Vojtesek, B.; Sparks, A.; Lane, D. P. Immunochemical Analysis of the Interaction of p53 with mdm2; Fine Mapping of the mdm2 Binding Site on p53 Using Synthetic Peptides. *Oncogene* **1994**, *9*, 2523−2529. For another approach to map the p53-binding site in the mdm2 protein, see: (b) Freedman, D. A.; Epstein, C. B.; Roth, J. C.; Levine, A. J. A Genetic Approach to Mapping the p53 Binding Site in the mdm2 Protein. *Mol. Med.* **1997**, *3*, 248−259.

(8) Böttger, A.; Böttger, V.; García-Echeverría, C.; Chène, P.; Hochkeppel, H. K.; Sampson, W.; Ang, K.; Howard, S. F.; Picksley, S. M.; Lane, D. P. Molecular Characterization of the mdm2-p53 Interaction. *J. Mol. Biol.* **1997**, *269*, 744−756.

(9) Böttger, V.; Böttger, A.; Howard, S. F.; Picksley, S. M.; Chene, P.; García-Echeverría, C.; Hochkeppel, H. K.; Lane, D. P. Identification of Novel mdm2 Binding Peptides by Phage Display. *Oncogene* **1996**, *13*, 2141−2147.

(10) (a) Kussie, P. H.; Gorina, S.; Marechal, V.; Elenbaas, B.; Moreau, J.; Levine, A. J.; Pavletich, N. P. Structure of the mdm2 Oncoprotein Bound to the p53 Tumor Suppresor Transactivation Domain. *Science* **1996**, *274*, 948−953. For additional structural papers related to p53, see: (b) Mittl, P. R. E.; Chène, P.; Grütter, M. G. Crystallization and Structure Solution of p53 (Residues 326−356) by Molecular Replacement Using an NMR Model as Template. *Acta Crystallogr.* **1998**, *D54*, 86−89. (c) Chène, P.; Mittl, P.; Grütter, M. In Vitro Structure−Function Analysis of the β-Strand 326−333 of Human p53. *J. Mol. Biol.* **1997**, *273*, 873−881. (d) Jeffrey, P. D.; Gorina, S.; Pavletich, N. P. Crystal Structure of the Tetramerization Domain of the p53 Tumor Suppressor at 1.7 angstroms. *Science* **1995**, *267*, 1498−1502. (e) Cho, Y.; Gorina, S.; Jeffrey, P. D.; Pavletich, N. P. Crystal Structure of a p53 Tumor Suppressor-DNA Complex: Understanding Tumorigenic Mutations. *Science* **1994**, *265*, 346−355.

(11) (a) Marshall, G. R.; Hodgkin, E. E.; Langs, D. A.; Smith, G. D.; Zabrocki, J.; Leplawy, M. T. Factors Governing Helical Preference of Peptides Containing Multiple α,α-Dialkyl Amino Acids. *Proc. Natl. Acad. Sci. U.S.A.* **1990**, *87*, 487−491. (b) Benedetti, E.; di Blasio, B.; Pavone, V.; Pedone, C.; Santini, A.; Crisma, M.; Valle, G.; Toniolo, G. Structural Versatility of Peptides from $C^{\alpha,\alpha}$-Dialkylated Glycines: Linear Ac_3c Homooligopeptides. *Biopolymers* **1989**, *28*, 175−184. (c) Toniolo, C.; Bonora, G. M.; Bavoso, A.; Benedetti, E.; di Blasio, B.; Pavone, V.; Pedone, G. Preferred Conformations of Peptides Containing α,α-Disubstituted α-Amino Acids. *Biopolymers* **1983**, *22*, 205−215.

(12) 1-Aminocyclopropanecarboxylic acid was selected to replace Gly^{25} due to its marked structural preferences for position $i + 2$ of type-I (I′) and type-II (II′) β-bends: Toniolo, C.; Benedetti, E. Structures of Polypeptides from α-Amino Acids Disubstituted at the α-Carbon. *Macromolecules* **1991**, *24*, 4004−4009.

(13) Wishart, D. S.; Sykes, B. D.; Richards, F. M. The chemical shift index: a fast and simple method for the assignment of protein secondary structure through NMR spectroscopy. *Biochemistry* **1992**, *31*, 1647−1651.

(14) Wüthrich, K. *NMR of proteins and nucleic acids*; John Wiley and Sons: New York, 1986.

(15) According to our model, the salt bridge between the phosphonate group and the amino group of the side chain of lysine is not buried, which would explain the relative modest increase in binding activity observed for this single amino acid replacement.

(16) Replacement of tryptophan by 5-substituted tryptophans has almost no effect in the binding activity, e.g., Ac-Met-Pro-Arg-Phe^{19}-Met-Asp-Tyr-Xxx-Glu-Gly-Leu^{26}-Asn-NH_2: $IC_{50} = 313$ nM, Xxx = Trp (entry 2, Table 1); $IC_{50} = 235$ nM, Xxx = 5-Me-Trp; and $IC_{50} = 25$ nM, Xxx = 6-Me-Trp.

(17) During the preparation of this manuscript, I. Massova and P. Kollman [(a) Massova, I.; Kollman, P. A. Computational Alanine Scanning to Probe Protein−Protein Interactions: A Novel Approach to Evaluate Binding Free Energies. *J. Am. Chem. Soc.* **1999**, *121*, 8133−8143] reported an impressive computational study of the p53/mdm2 interaction. These authors have calculated the binding free energy changes associated with various structural modifications of the amino acid stretch of p53 in interaction with mdm2. In particular and in excellent agreement with the biological data shown in this Communication, their calculations suggest that adding a methyl substituent in $C_{\eta 2}$ of Trp^{23} (in our nomenclature, $C_{\eta 2}$ corresponds to position 6 of the indole) should improve binding affinity. For other examples of p53/hdm2 antagonists, see: (b) Luke, R. W. A.; Hudson, K.; Hayward, C. F.; Fielding, C.; Cotton, R.; Best, R.; Giles, M. B.; Veldman, M. H.; Griffiths, L. A.; Jewsbury, P. J.; Breeze, A. L.; Embrey, K. J. Design and synthesis of small molecule inhibitors of the mdm2-p53 interaction as potential antitumor agents. *Proc. Am. Assoc. Cancer Res.* **1979**, *39*, 622. (c) Di Domenico, R.; Hansen, S.; Kaluza, B.; Menta, E.; Schumacher, R. Derivatives of phenoxy acetic acid and phenoxymethyltetrazole having antitumor activity. EP 947 494 A1, F. Hoffmann-La Roche AG.

JM990966P